

**Point-source moment tensor inversion via a Bayesian hierarchical inversion with 2D-structure uncertainty: Implications for the 2009-2017 DPRK nuclear tests**

Jinyin Hu<sup>1</sup>, Thanh-Son Phạm<sup>1</sup> and Hrvoje Tkalčić<sup>1</sup>

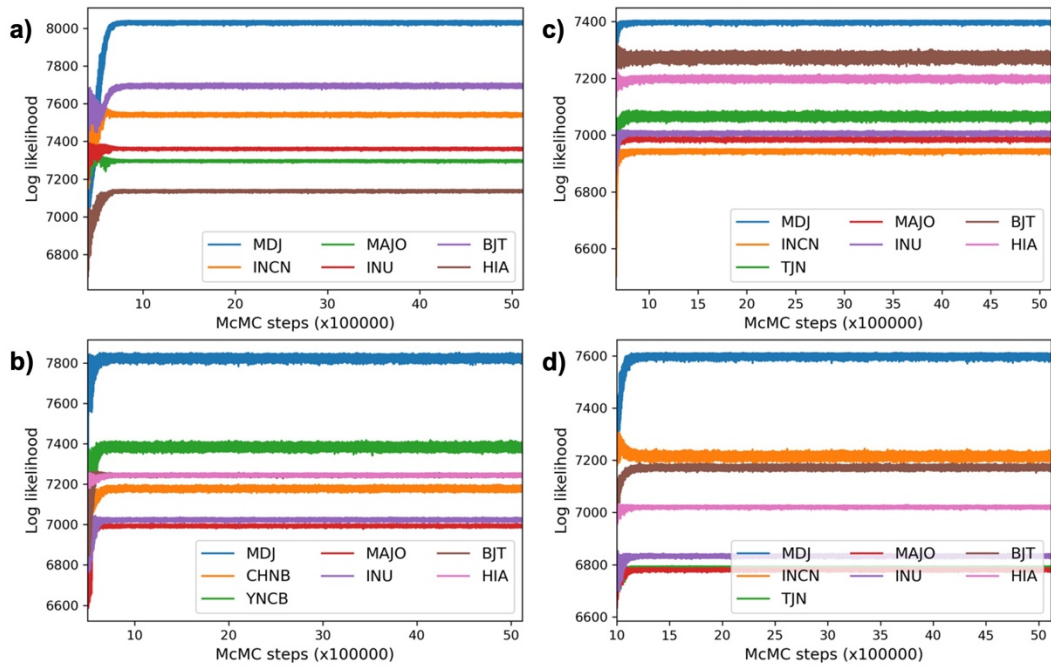
<sup>1</sup>Research School of Earth Sciences, The Australian National University, Canberra, ACT, Australia

**Contents of this file**

Figures S1 to S4

**Introduction**

The information included Figures S1 to S4 expand the discussion briefly discussed in the main text.



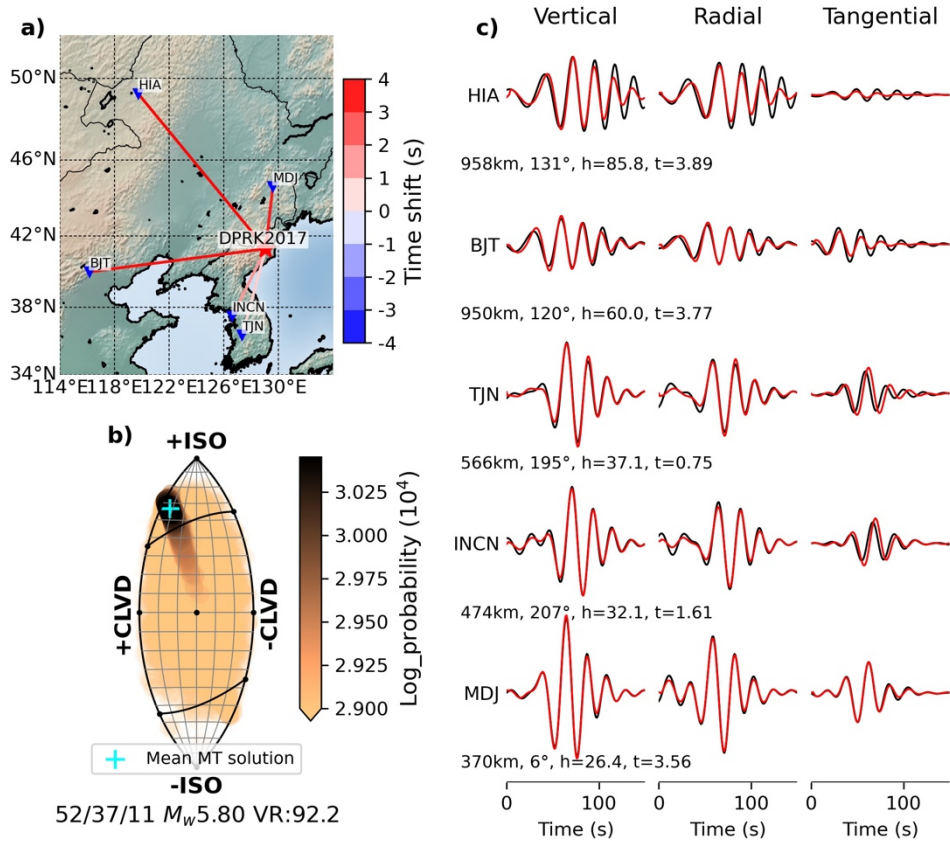
27

28 **Figure S1.** Log-likelihood calculated for each station during MT inversions for the (a) DRPK2009,  
 29 (b) DPRK2013, (c) DPRK2016a, and (d) DPRK2016b tests, respectively. Most burn-in steps are  
 30 discarded to illustrate the likelihood function in the convergence stage.

31

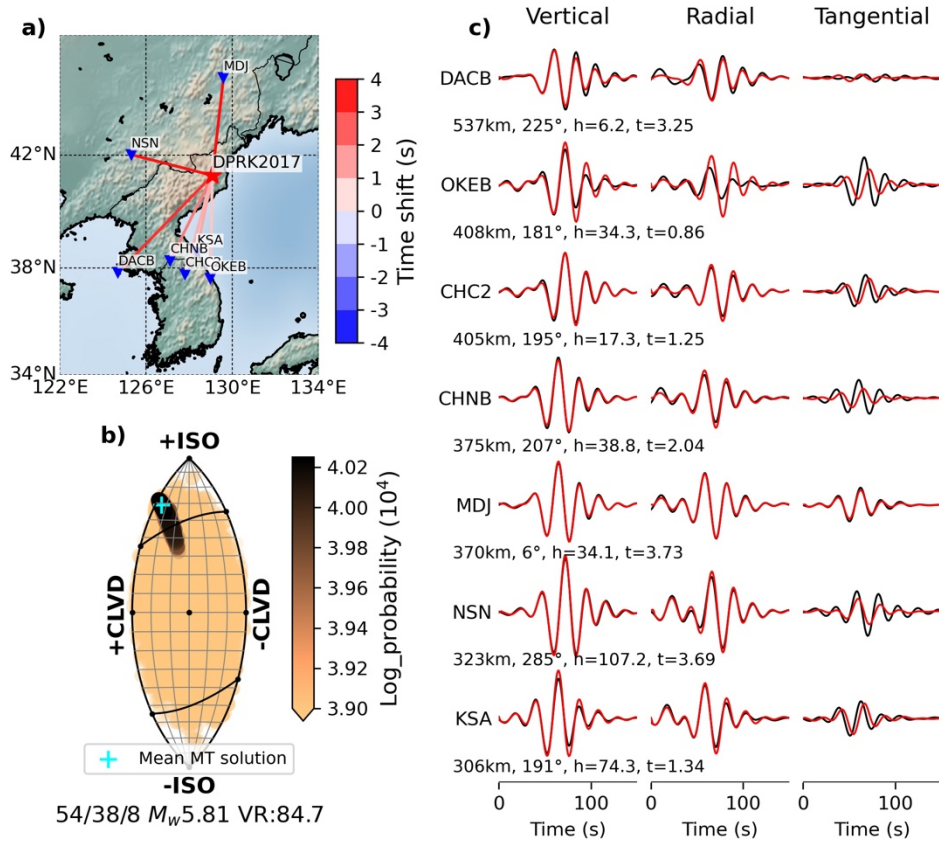
32

33

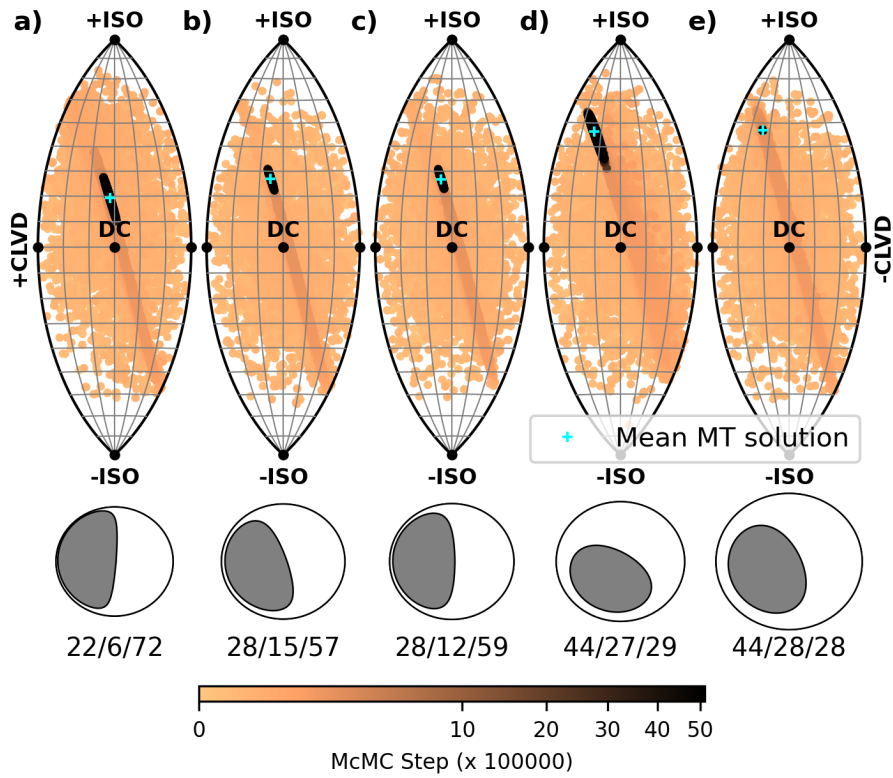


34

35 **Figure S2.** MT Solutions were obtained by hierarchical Bayesian inversion considering  
 36 uncorrelated noise and 2D structural error when removing two stations in Japan. (a) Map of region  
 37 showing five stations and the recovered station-based time shift. (b) The source-type lune diagram  
 38 shows MT solutions' evolution during the inversion. The cyan cross marks the source type of the  
 39 mean MT solution. The color bar is used for log- probability. All log-probability under  $2.7 \times 10^4$  is  
 40 set to be black to visualize the later stage of the inversion better. The numbers beneath are percent  
 41 ISO, CLVD, DC, moment magnitude of the mean MT, and the waveform fit variance reduction for  
 42 the mean MT. (c) Waveform fit between the observed (black) and predicted waveforms (red) from  
 43 mean MT plot in (b). The numbers below each row are source-station distance, azimuth, recovered  
 44 station-specific noise parameters, and time shifts, respectively.



45  
 46 **Figure S3.** MT solutions were obtained by hierarchical Bayesian inversion considering  
 47 uncorrelated noise and 2D structural error using another dataset. (a) Map of region showing seven  
 48 stations and the recovered station-based time shifts. (b) The source-type lune diagram shows MT  
 49 solutions' evolution during the inversion. (c) Waveform fit between observed and predicted  
 50 waveforms from mean MT plot in (b). See caption of Figure S2 for more details.



51

52 **Figure S4.** Lune diagram of source type of MT solutions when fixing the noise strength to the  
 53 same as pre-event ambient noise for five DPRK tests from 2009 to 2017 with panels (a)-(e),  
 54 respectively. See caption of Figure 9 for details.

55